

1-1-1976

Delay effects in a pressure vessel material - 5083-0 aluminum.

Kenneth A. Wnek

Follow this and additional works at: <http://preserve.lehigh.edu/etd>



Part of the [Mechanical Engineering Commons](#)

Recommended Citation

Wnek, Kenneth A., "Delay effects in a pressure vessel material - 5083-0 aluminum." (1976). *Theses and Dissertations*. Paper 2073.

This Thesis is brought to you for free and open access by Lehigh Preserve. It has been accepted for inclusion in Theses and Dissertations by an authorized administrator of Lehigh Preserve. For more information, please contact preserve@lehigh.edu.

DELAY EFFECTS IN A
PRESSURE VESSEL MATERIAL - 5083-O ALUMINUM

BY
KENNETH A. WNEK

A Thesis
Presented to the Graduate Committee
of Lehigh University
in Candidacy for the Degree of
Master of Science

in
Mechanical Engineering

Lehigh University

1976

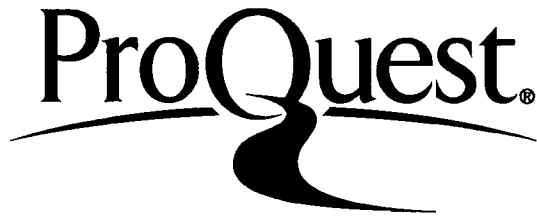
ProQuest Number: EP76346

All rights reserved

INFORMATION TO ALL USERS

The quality of this reproduction is dependent upon the quality of the copy submitted.

In the unlikely event that the author did not send a complete manuscript and there are missing pages, these will be noted. Also, if material had to be removed, a note will indicate the deletion.



ProQuest EP76346

Published by ProQuest LLC (2015). Copyright of the Dissertation is held by the Author.

All rights reserved.

This work is protected against unauthorized copying under Title 17, United States Code
Microform Edition © ProQuest LLC.

ProQuest LLC.
789 East Eisenhower Parkway
P.O. Box 1346
Ann Arbor, MI 48106 - 1346

This thesis is accepted and approved in partial fulfillment of the requirements for the degree of Masters of Science.

9/14/76

(date)

Professor in Charge

Chairman of Department

ACKNOWLEDGMENTS

The author gratefully acknowledges the instruction, guidance and friendship of his advisor, Professor Richard Roberts. Gratitude is also expressed to the Senior Staff and fellow graduate students in the Department of Mechanical Engineering, and Department of Metallurgy and Materials Science at Lehigh, many of whom have contributed technical information and practical assistance during the course of this study.

The author also wishes to thank Eugene Kozma, technician for Materials Research Center at Lehigh, for his technical assistance during the experimental portion of this research, and special thanks to Miss Joan Svirzofsky for typing this thesis.

TABLE OF CONTENTS

	PAGE
Title Page	i
Certificate of Approval.	ii
Acknowledgement.	iii
Table of Contents.	iv
List of Tables	v
List of Figures.	vi
Abstract	1
Introduction	2
Experimental Procedure	4
Test Results	5
Interaction Free Behavior	5
Delay Test Groups I, II, III ($\Delta K = 13.2, 19.8, 26.4 \text{ MPa}\sqrt{\text{m}}$; 50% O.L.)	7
Delay Test Groups IV, V, VI, and VII ($\Delta K = 13.2, 19.8 \text{ MPa}\sqrt{\text{m}}$; 75 and 100% O.L.)	8
Analysis of Scatter of Delay Results.	8
Discussion	9
Conclusions.	12
References	30
Vita	31

LIST OF TABLES

	PAGE
Table 1. Summary of Delay Results for 50% Overloads	14
Table 2. Summary of Delay Results for 75% Overloads	15
Table 3. Summary of Delay Results for 100% Overloads. . . .	16
Table 4. Summary of Calculated Bounds and Experimental Values for Delay Cycles.	17

LIST OF FIGURES

	PAGE
Figure 1. Stress intensity wave form with interaction . . .	18
Figure 2. Dimensions of compact tension specimens	19
Figure 3. Constant load wave form	20
Figure 4. Schematic of environmental control system for deionized water	21
Figure 5. Load shedding process for constant ΔK tests . . .	22
Figure 6. Growth rate as a function of stress intensity range	23
Figure 7. Growth rate as a function of stress intensity range for tests run in deionized water.	24
Figure 8. Schematic of a growth rate curve resulting from a single overload	25
Figure 9. Comparison of a^* and a_c^*	26
Figure 10. Band of Growth rate - Distance from overload results	27
Figure 11. Comparison of growth rate vs. distance from overload results for 50, 75, 100% overloads . . .	28
Figure 12. Cycles of delay versus ΔK level for 50, 75 and 100 percent overloads	29

ABSTRACT

The effect of 50, 75, and 100 percent overloads on fatigue crack propagation in 5083-0 aluminum alloy was investigated in this study. Typical tests consisted of fatiguing compact tension specimens at constant stress intensity range levels of 13.19, 19.78, and 26.38 MPa \sqrt{m} while maintaining the minimum K level at zero. A single overload was manually applied at a fixed crack length in each test, after which the original loading program at the baseline ΔK level was resumed.

As a result of these peak loads, retardation of crack growth rates occurred, and the amount of retardation was found to increase with increasing overload magnitude. Cycles of delay ranged from 4.45×10^4 cycles for $\Delta K = 13.19$ MPa \sqrt{m} , 50% overload tests, to 80.1×10^4 cycles for $\Delta K = 26.38$ MPa \sqrt{m} , 75% overload tests. Also, the size of the affected region of delay compared well with calculated plastic zone sizes.

Constant ΔP tests were also run on the 5083-0 alloy to establish baseline $da/dN-\Delta K$ data, and develop an estimate of the scatter band for growth rates. Using the bounds of a 95% confidence interval for the results, the scatter of delay data was found to result primarily from the variance of growth rates between identical tests. Scatter of experimental delay results for most tests fell reasonably within limits calculated using the $da/dN-\Delta K$ confidence interval.

INTRODUCTION

The rate of crack propagation in materials subjected to constant amplitude loading is adequately described by recent fracture mechanics based theories (1). These theories play a major role in the design of many structures under cyclic loading. Pressure vessels, for instance, may undergo many cycles of pressurizing and depressurizing, and it is very important to be able to predict flaw growth rates and critical flaw conditions. Aircraft wings and bridges are also examples of engineering systems subjected to cyclic loading. With the use of fracture mechanics in their design, catastrophic failures can in many cases be avoided.

One popular theory for the estimation of sub-critical crack growth due to constant amplitude loading has been introduced by Paris and Erdogan (2). The relationship takes the exponential form

$$da/dN = C(\Delta K)^m \quad [1]$$

where a = crack length, N = number of cycles, ΔK = stress intensity range, and C and m are proposed to be constants dependent upon environment, material properties, and test parameters. This theory, however, fails to predict crack growth from loading programs containing interactions such as overloads. See Figure 1. It has been found in previous works (3, 4, 5), and will be further investigated in this study, that the application of an overload to a constant amplitude loading pattern brings about a retardation

of fatigue crack propagation. With such load interactions, Trebules (3) and von Euw (4) have found that in 2024-T3 aluminum, crack growth rates decrease considerably, and in some instances almost to the point of complete crack arrest. They also found that increasing the percentage of overload or baseline stress intensity or both, brings about a larger effect. Increasing the number of overload cycles can also bring about larger delay effects. Studies on thickness effects by Wei (5) and Mills (6) have further shown that delay is dependent on state of stress.

Delay phenomena has been attributed to such effects as change in crack tip geometry, residual stress ahead of the crack front, and crack closure. It has been postulated that upon the application of an overload, residual compressive stresses form which act to reduce crack growth rates. Blunting of the crack tip has also been suggested as a possible cause of delay effects. The more recent proposal by Elber (7), crack closure, suggests that residual tensile displacements interfere along the crack surface in the wake of the crack front. The result is a reduction in the effective stress intensity range.

Previous investigation on the subject of delay of fatigue crack propagation due to overloads, has shown variance of delay results. von Euw (4) reported delay cycles for identical tests which varied by about a factor of two, and it was also evident from his work that the scatter of results depended upon the magnitude of the overload and base stress intensity level; higher loads bring

about more scatter.

The objective of this study is to investigate the fatigue and delay properties of 5083-0 aluminum. This material is widely used in cryogenic applications such as pressure vessels. Whether a proof load will increase or decrease the service life of these structures can be a crucial question.

EXPERIMENTAL PROCEDURE

The material used in this study was 5083-0 aluminum alloy: (0.4% Si, 0.4% Fe, 0.1% Cu, 0.3-1.0% Mn, 4.0-4.9% Mg, 0.05-0.25% Zn, 0.15% Ti), 6.34 mm thick, with a nominal yield strength and ultimate strength of 124 MN/m² and 276 MN/m² respectively. The material was cut into compact tension specimens with dimensions as in Trebules (3) work, Figure 2.

Fatigue testing of the specimens was done on an 89 kN electrohydraulic closed loop testing machine, with a laterally moving microscope for measuring crack extension. A sinusoidal loading function with a frequency of 20 Hz was used for all tests.

In the first part of the test program, constant load tests were run at $\Delta P = 4295\text{N}$ (Figure 3), to develop baseline $da/dN - \Delta K$ data, and to estimate typical scatter in growth rate data for 5083-0 aluminum. All tests were done in air at room temperature and approximately 50-75 percent relative humidity. Tests were also run in a deionized water environment to examine the effects of moisture on crack growth rates. To achieve this environment, a

sealed chamber was attached to the front and back of each specimen, enclosing the notch and crack region. Water was then passed into the front chamber and allowed to flow into the rear chamber through a small hole in the specimen. This hole was drilled far from the crack region so that no interaction would occur. See Figure 2. A schematic of this system is shown in Figure 4.

In the second portion of the test program, tests were run at constant stress intensity range levels, ΔK . To achieve this the loads were shed after increments of 0.2 mm of crack growth. This particular load shedding program was necessary to keep the stress intensity range constant within one percent. See Figure 5.

A single overload was applied to each specimen when a crack length of 24 mm was reached. This initial crack length was used to insure enough data for establishing interaction free behavior for each specimen. After the overload, the original loading program was resumed at the base stress intensity level corresponding to the new crack length. See Figure 1.

TEST RESULTS

INTERACTION FREE BEHAVIOR

In the constant load range portion of the test program, crack growth rates were determined by taking the slopes of tangent lines drawn at different points to the a vs. N curves produced from each test. The stress intensity level corresponding to each growth rate was calculated using the equation from ASTM Standard

E399-72 (8)

$$\Delta K = \frac{\Delta P}{BW^{1/2}} \left(29.6 \left(\frac{a}{W}\right)^{1/2} - 185.5 \left(\frac{a}{W}\right)^{3/2} + 655.7 \left(\frac{a}{W}\right)^{5/2} - 1017.0 \left(\frac{a}{W}\right)^{7/2} + 638.9 \left(\frac{a}{W}\right)^{9/2} \right) \quad [2]$$

which relates the ΔK level to load range, specimen geometry, and crack length.

A log-log plot of the da/dN - ΔK values was then constructed and an equation of the form of equation [1] was fit to the data using a least squares regression analysis. This is quite simple since Paris' equation [1] linearizes upon taking logarithms as shown below.

$$\begin{aligned} da/dN &= C(\Delta K)^m \\ \log(da/dN) &= \log C + m \log \Delta K \\ \downarrow \quad \quad \downarrow \quad \quad \downarrow \\ Y &= B + mX \end{aligned} \quad [3]$$

Bounds for the scatter band were formed by calculating a 95 percent confidence interval for growth rates corresponding to particular ΔK values. This was done by adding to or subtracting from equation (3) found through the regression analysis, a factor of the form 0.96σ ; σ being the standard deviation of the dependent variable. The log-log plot discussed above is shown in Figure 6.

The tests run in deionized water produced growth rates slightly higher than those in air showing the possibility of a small humidity effect on crack propagation. Figure 7 shows the da/dN vs. ΔK relationship for these tests as compared with air

tests.

DELAY TEST GROUPS I, II, AND III ($\Delta K = 13.2, 19.8, 26.4 \text{ MPa}\sqrt{\text{m}}$;
50% O.L.)

In these test groups stress intensity ranges of 13.2, 19.8, and 26.4 $\text{MPa}\sqrt{\text{m}}$ were used to precrack the specimens to a crack length of 24 mm. At this point, one 50% overload was applied to each specimen after which normal fatigue loading at the base ΔK level was resumed. Each test was terminated when the crack began growing at a stable rate close to that observed before the overload. The delay results for these groups are shown in Table I, and definitions of delay parameters are shown in Figure 8.

As suggested by von Euv (4), the region affected by an overload should be approximately equal to the size of the plastic zone created by the high load. The radius of the plastic zone is found from the equation (4)

$$r_y = \frac{1}{d\pi} \left(\frac{\Delta K_{OL}}{\sigma_{ys}} \right)^2 \quad [4]$$

and length of the delay region is simply twice the plastic zone radius, or

$$a_c^* = 2r_y \quad [5]$$

The value d reflects the amount of shear fracture as measured on the specimen crack surface, and varies from 2 for plane stress to 6 for plane strain. Intermediate values of d for mixed mode

fracture can be determined using the following equation

$$\frac{l}{d} = \left(\frac{\% \text{ flat}}{100} \times \frac{l}{6} + \frac{\% \text{ shear}}{100} \times \frac{l}{2} \right) \quad [6]$$

Figure 9 is a graph comparing the calculated affected region a_c^* , to the actual affected region a^* , determined experimentally. It should be noted that negligible shear appeared on the crack surfaces of most of the tests, revealing plane strain conditions, and thus a d value of 6 was used.

DELAY TEST GROUPS IV, V, VI, AND VII ($\Delta K = 13.2, 19.8 \text{ MPa}\sqrt{\text{m}}$
75 and 100% O.Ls.)

These specimens were loaded for ΔK levels of 13.2 and 19.8 $\text{MPa}\sqrt{\text{m}}$ just as in test groups I, II, and III. One 75 percent overload was applied to each specimen in groups IV and V, and one 100 percent overload to each specimen in groups VI and VII. These overloads were applied at crack lengths of 24 mm, and then the base ΔK levels were resumed. The load interaction results for these groups are found in Tables 2 and 3. It should be noted that extensive deformation of the crack tip and permanent opening of the crack resulted from the 100 percent overloads.

ANALYSIS OF SCATTER OF DELAY RESULTS

It is believed that the scatter of delay results is primarily due to the variance of crack growth rates at a particular stress intensity level. To investigate this, crack growth rates within the delay regions were measured and plotted against distance from point of overload for each delay test. Each test group

yielded results in the form of a band as shown in Figure 10.

The average variation of crack growth rate with distance from overload was approximated by a series of straight line segments through the middle of the band, the equation of these lines being some function of crack length, or

$$da/dN = f(a) \quad [7]$$

The growth rates along these lines were assumed to correspond to the average growth rates found along the line of the log-log plot of da/dN vs. ΔK determined by the regression analysis. Then using the bounds of the 95 percent confidence interval for the da/dN vs. ΔK data, upper and lower crack growth rate limits were determined and used to find upper and lower bounds on $f(a)$. Remembering that the upper bound of growth rates yields the lower bound of cycles of delay, the integration of equation [7] was done as follows

$$\left. \begin{aligned} \left(\frac{da}{dN}\right)_{\text{upper}} &= f(a)_{\text{upper}} \\ N_{\text{lower}} &= \int \frac{da}{f(a)_{\text{upper}}} \end{aligned} \right| \left. \begin{aligned} \left(\frac{da}{dN}\right)_{\text{lower}} &= f(a)_{\text{lower}} \\ N_{\text{upper}} &= \int \frac{da}{f(a)_{\text{lower}}} \end{aligned} \right. \quad [8]$$

Calculated upper and lower limit delay cycle values are tabulated with the actual experimental values in Table 4.

DISCUSSION

The results listed in Table 4 show that the variance of growth rates from test to test at a particular ΔK level, have a

large effect on delay results. For most of the delay test groups, the number of cycles of delay determined experimentally fall reasonably within the calculated bounds. Although for some of the tests the delay cycles fall slightly outside the bounds, it must be remembered that many approximations and assumptions were made which would reduce the accuracy of the procedure used. Perhaps a more precise curve fit through the band of growth rate vs. distance from overload data, rather than straight line segments would adjust the bounds to cover more experimental results.

The crack growth rate vs. ΔK results from the deionized water tests could have been used to provide the upper bound for the analysis. However, it is believed that since most of the constant ΔP tests were done on different days, enough variance of relative humidity was already included in the scatter, and the water data was not needed. Also, looking at Figure 7, we see that the results in the water environment did not differ much with the upper bound air tests, showing that moisture effects in these tests were negligible. It should also be noted that constant ΔP test results from this study compare well with those found by Kelsey, Nordmark, and Clark (8). C and m values for their similar tests were approximately 3.1×10^{-8} mm/cycle and 3.51 respectively as compared to values from the tests in this study; 2.06×10^{-8} mm/cycle and 3.54.

In some delay test groups differences in delay zone sizes were evident, especially in those groups with high ΔK levels and

high overloads where actual measured zones varied in size by as much as 6 mm. This fact may hint to the possibility of changes in stress state, and a few fracture surfaces did in fact reveal a small amount of mixed mode fracture.

In test group VII, the experimentally determined cycles of delay did not fall within the bounds calculated. Instead, one test (specimen #36) resulted in 80.1×10^4 cycles of delay, almost twice the upper bound value. In another test (specimen #21), 7.2×10^4 cycles were measured which is about one-third the lower bound. Delay zone sizes for these two tests measured 12.00 mm for specimen #36 and 7.6 mm for specimen #21, as opposed to the calculated value of 10.75 mm for plane strain conditions.

Experiments by Wei (5) and Mills (6) on thickness effects on delay, have shown that stress state changes can bring about large differences in the number of delay cycles. More delay was found to occur under plane stress conditions than under plane strain, and the variance of results could be as high as a factor of 3. Although most of the tests in this study did not reveal gross shear fracture, slight differences in stress state could account for scatter in the high overload tests, where small amounts of slant fracture were detected. Also, plastic zone sizes calculated using equation [4] were found to exceed specimen thickness thus revealing that plane stress conditions prevailed.

Another important observation is from the crack growth rate vs. distance from overload curves for 50, 75, and 100 percent

overloads. See Figure 11. These curves show that smaller growth rates result from higher overloads. Since it is at the troughs of these curves where the largest portion of the delay cycles occurs, it is evident that higher overloads will produce longer delay periods. See Figure 12. The critical point here is that small differences in minimum growth rates between specimens run at the same ΔK levels and percent overloads, can bring about large differences in delay cycles. In comparing with the results of Trebules (3) and von Euw (4) it is noticed that the trough width, or amount of crack growth at the minimum rate for tests in this study are much larger. Regions of crack growth at the minimum rate for these tests range between 2 and 6 mm, whereas in the published results, only a single point of minimum crack growth rate is evident.

From Tables 1, 2, and 3 it might be noticed that tests with smaller initial growth rates before the overload, in general produce longer delay periods. Remembering that in the delay zone, the smaller growth rates produce the longer delay periods, there may also be some connection between growth rates before overload and delay cycles. However, not enough data was collected in this study to investigate this point.

CONCLUSIONS

The following conclusions can be made on the basis of the experimental results from this study:

1. The application of a single proof load to structures of 5083-0 Aluminum, such as pressure vessels, can bring about retardation of flaw growth.
2. The number of delay cycles due to a single overload increases with the magnitude of the overload.
3. Smaller minimum growth rates within the delay region result from higher magnitude overloads.
4. Delay zones or affected regions compare well with calculated plastic zone sizes.
5. The experimental scatter in number of cycles of delay can be accounted for in most tests by variation of growth rates at a particular ΔK level.
6. At high loads, the transition from plane strain to plane stress could produce large differences in delay results.

It is recommended that future work be done on the effects

of

1. Fatigue crack propagation scatter on delay cycles.
2. Transition of plane strain to plane stress on delay cycles.

TABLE I. SUMMARY OF DELAY RESULTS FOR 50% OVERLOADS

(The definitions of a_1 , a_2 , a^* , N^* , and N_D^* are found in Figure #8)

Specimen No.	ΔK MPa \sqrt{m}	a_1 (mm/cycle) $\times 10^{-4}$	a_2 (mm/cycle) $\times 10^{-4}$	a^* mm	a_c^* mm	N^* Cycles $\times 10^4$	N_D^* Cycles $\times 10^4$
10	13.19	2.04	2.00	3.70	2.69	5.00	3.40
13	13.19	2.05	1.40	3.30	2.69	4.60	2.60
17	19.78	3.33	3.53	6.20	6.06	4.45	3.05
18	19.78	5.14	4.32	5.50	6.06	2.95	1.85
37	19.78	3.33	3.50	5.85	6.06	6.60	4.60
39	19.78	3.51	3.78	6.00	6.06	4.40	2.80
43	26.38	8.39	11.80	9.50	10.75	3.75	2.95
11	26.38	8.00	9.09	7.00	10.75	2.30	2.20
00	26.38	10.00	6.83	7.30	10.75	2.80	2.20

TABLE 2. SUMMARY OF DELAY RESULTS FOR 75% OVERLOADS

Specimen No.	ΔK MPa \sqrt{m}	\dot{a}_1 (mm/cycle) $\times 10^{-4}$	\dot{a}_2 (mm/cycle) $\times 10^{-4}$	a^* mm	a_c^* mm	N^* Cycles $\times 10^4$	N_D^* Cycles $\times 10^4$
1	13.19	2.08	0.96	4.00	3.66	9.10	5.00
2	13.19	2.27	1.14	4.40	3.66	9.80	6.00
23	13.19	3.25	2.69	4.90	3.66	9.30	7.80
30	13.19	2.30	2.04	5.50	3.66	10.60	7.90
20	19.78	6.20	5.95	13.00	8.25	15.30	13.10
24	19.78	5.00	2.94	9.00	8.25	10.80	7.70
38	19.78	3.50	2.00	8.00	8.25	16.85	12.85
40	19.78	4.40	2.95	8.00	8.25	10.50	6.20
44	19.78	4.28	2.88	8.80	8.25	16.00	11.40

TABLE 3. SUMMARY OF DELAY RESULTS FOR 100% OVERLOADS

Specimen No.	ΔK MPa \sqrt{m}	\dot{a}_1 (mm/cycle) $\times 10^{-4}$	\dot{a}_2 (mm/cycle) $\times 10^{-4}$	a^* mm	a_c^* mm	N^* Cycles $\times 10^4$	N_0^* Cycles $\times 10^4$
7	13.19	2.13	2.00	4.00	4.79	28.50	26.75
8	13.19	1.76	0.22	2.60	4.79	17.00	4.00
25	13.19	2.67	1.53	10.00	4.79	35.00	26.90
9	19.78	4.70	2.56	6.00	10.75	10.00	7.60
21	19.78	4.57	2.14	7.60	10.75	7.20	4.70
36	19.78	3.92	2.00	12.00	10.75	80.10	74.00
41	19.78	3.29	2.80	11.60	10.75	27.50	23.55

TABLE 4. SUMMARY OF CALCULATED BOUNDS AND
EXPERIMENTAL VALUES FOR DELAY CYCLES

Test	Calculated Bounds ($\times 10^4$ cycles)	Experimental Results ($\times 10^4$ cycles)
$\Delta K = 13.2 \text{MPa}\sqrt{\text{m}}$, 50% O.L.	$3.4 < N < 8.0$	5.00 4.60
$\Delta K = 19.8 \text{MPa}\sqrt{\text{m}}$, 50% O.L.	$3.9 < N < 9.3$	4.45 2.95 6.60 4.40
$\Delta K = 26.4 \text{MPa}\sqrt{\text{m}}$, 50% O.L.	$2.6 < N < 6.0$	3.75 2.80 2.80
$\Delta K = 13.2 \text{MPa}\sqrt{\text{m}}$, 75% O.L.	$6.1 < N < 14.2$	9.10 9.80 9.30 10.60
$\Delta K = 19.8 \text{MPa}\sqrt{\text{m}}$, 75% O.L.	$8.4 < N < 19.7$	15.30 10.80 16.85 10.50 16.00
$\Delta K = 13.2 \text{MPa}\sqrt{\text{m}}$, 100% O.L.	$17.0 < N < 38.5$	28.50 17.00 35.80
$\Delta K = 19.8 \text{MPa}\sqrt{\text{m}}$, 100% O.L.	$24.6 < N < 51.2$	10.00 7.20 80.10 27.50

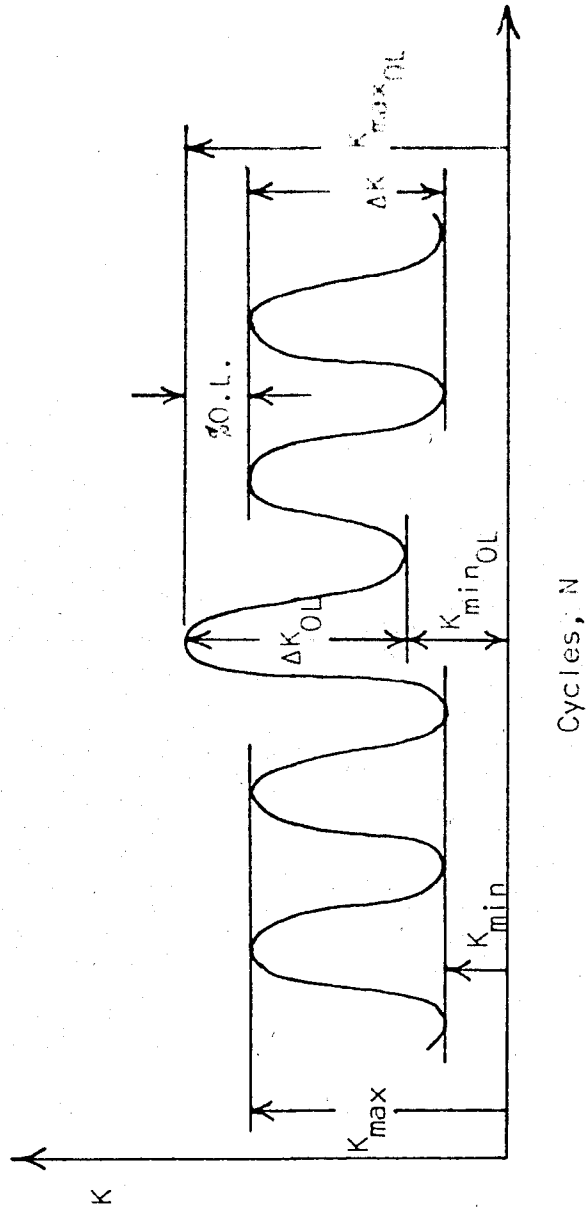
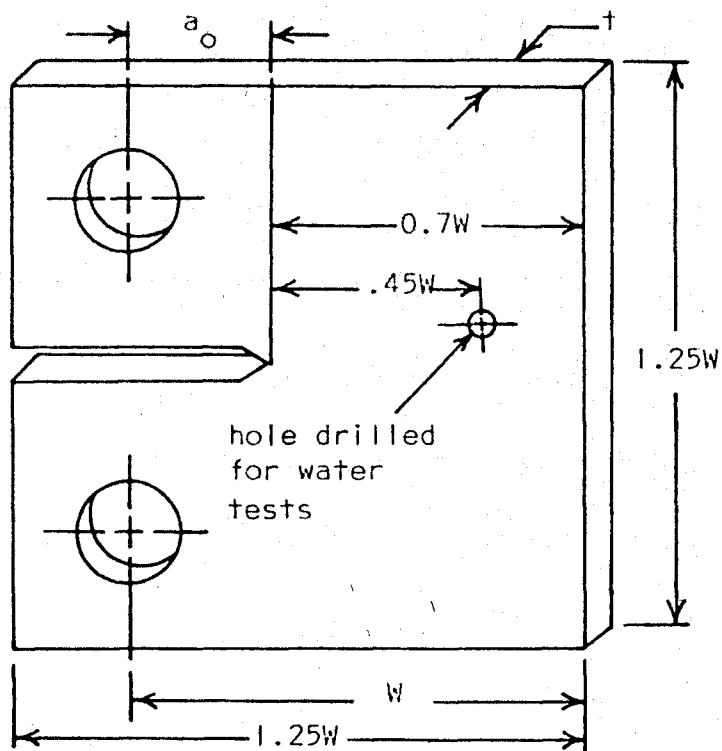


FIGURE 1. STRESS INTENSITY WAVEFORM WITH INTERACTION.



$W = 63.50\text{mm}$
 $a_0 = 19.05\text{mm}$
 $t = 3.18\text{mm}$

FIGURE 2. DIMENSIONS OF COMPACT TENSIONS SPECIMENS.

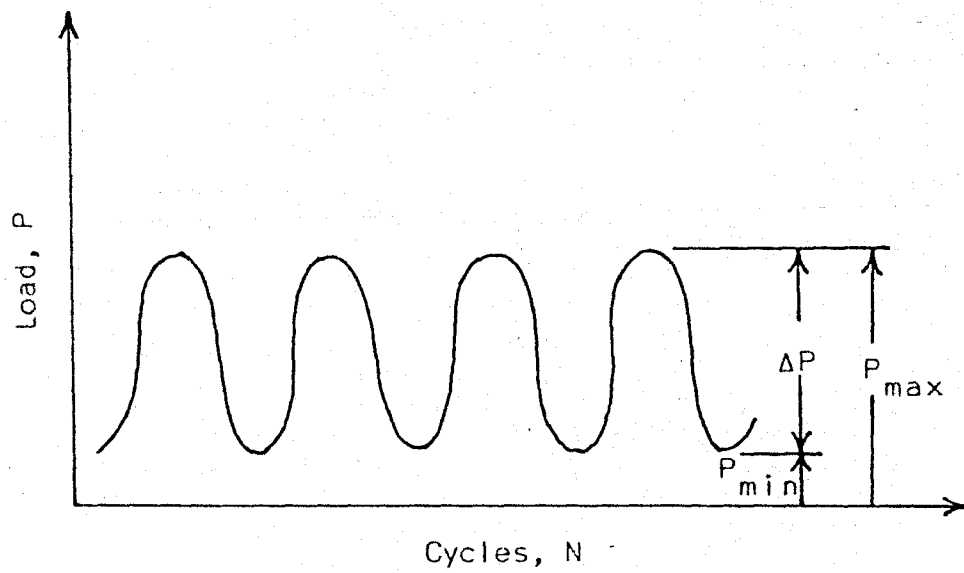


FIGURE 3. CONSTANT LOAD WAVEFORM.

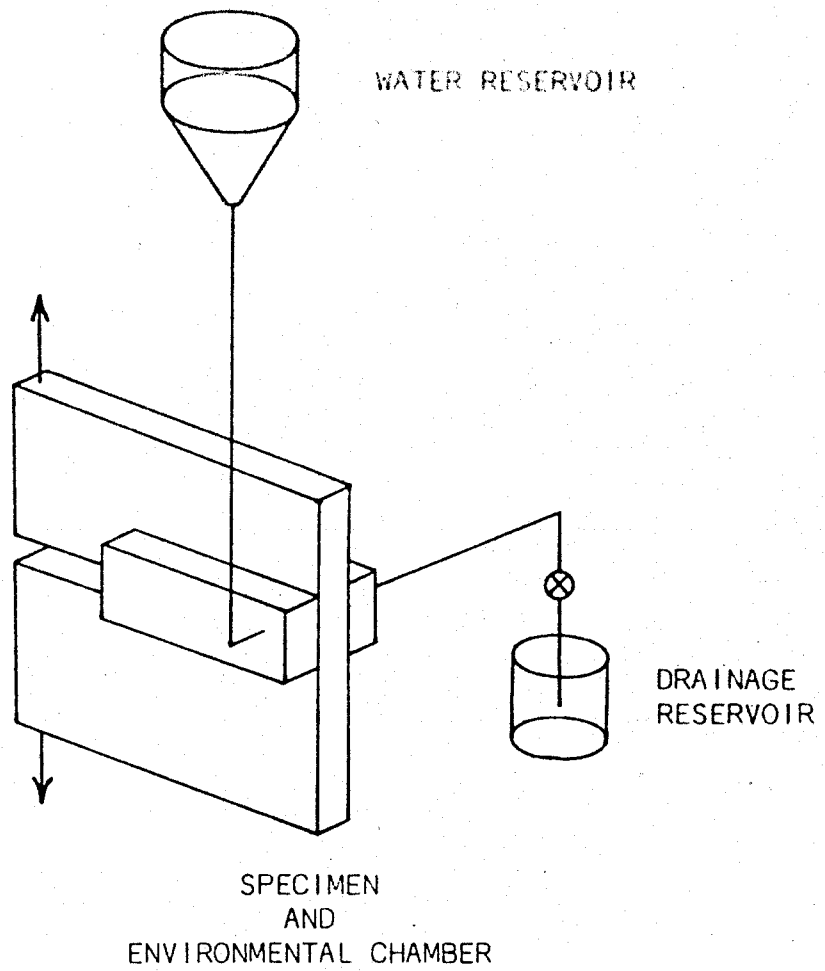


FIGURE 4. SCHEMATIC OF ENVIRONMENTAL CONTROL SYSTEM FOR DEIONIZED WATER.

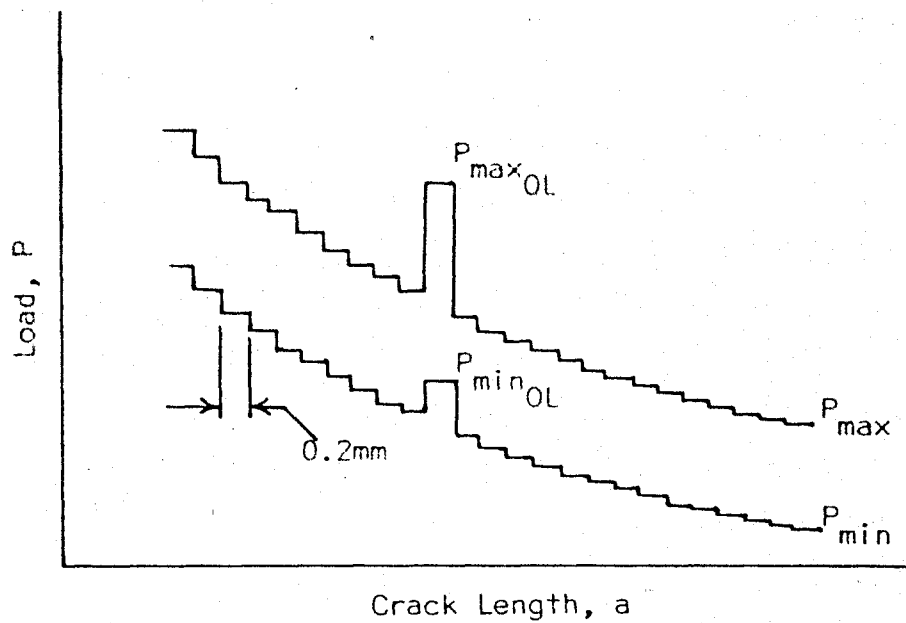


FIGURE 5. LOAD SHEDDING PROCESS FOR CONSTANT ΔK TESTS.

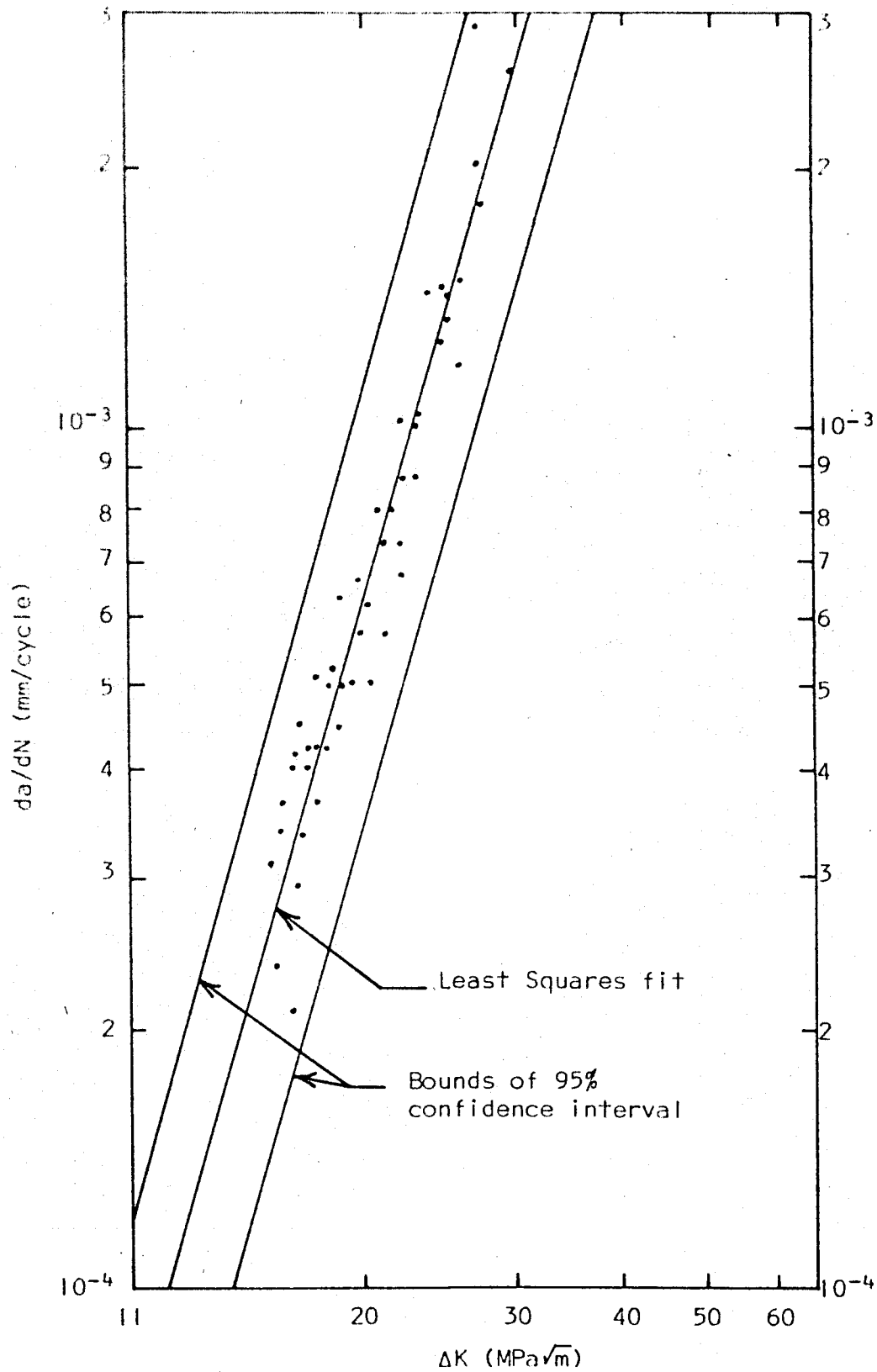


FIGURE 6. GROWTH RATE AS A FUNCTION OF STRESS INTENSITY RANGE. (from least squares fit, $da/dN = 2.06 \times 10^{-8} \Delta K^{3.54}$ S.I. units)

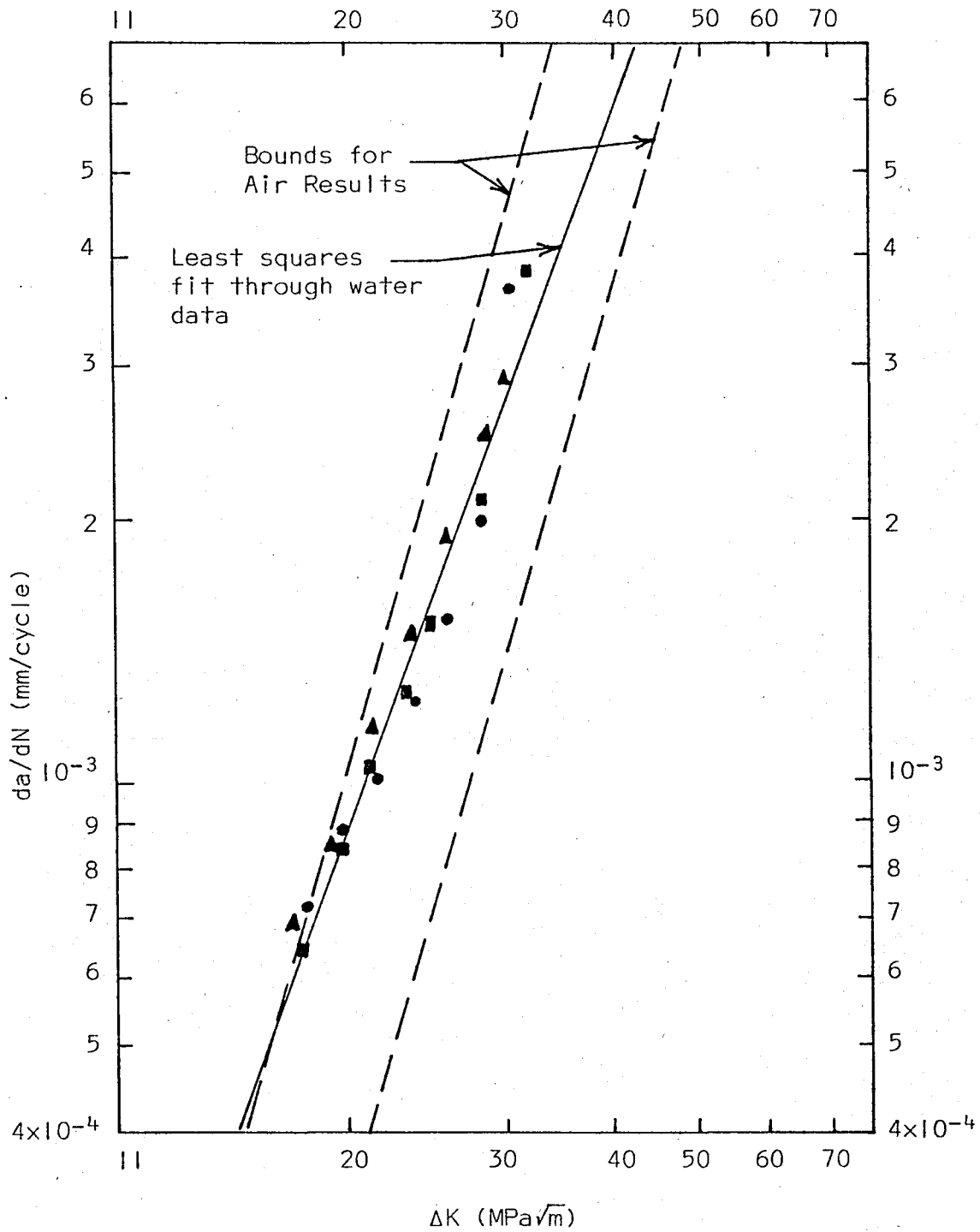


FIGURE 7. GROWTH RATE AS A FUNCTION OF STRESS INTENSITY RANGE FOR TESTS RUN IN DEIONIZED WATER. (from least squares fit, $da/dN = 8.15 \times 10^{-6} \Delta K^{2.74}$ S.I. units)

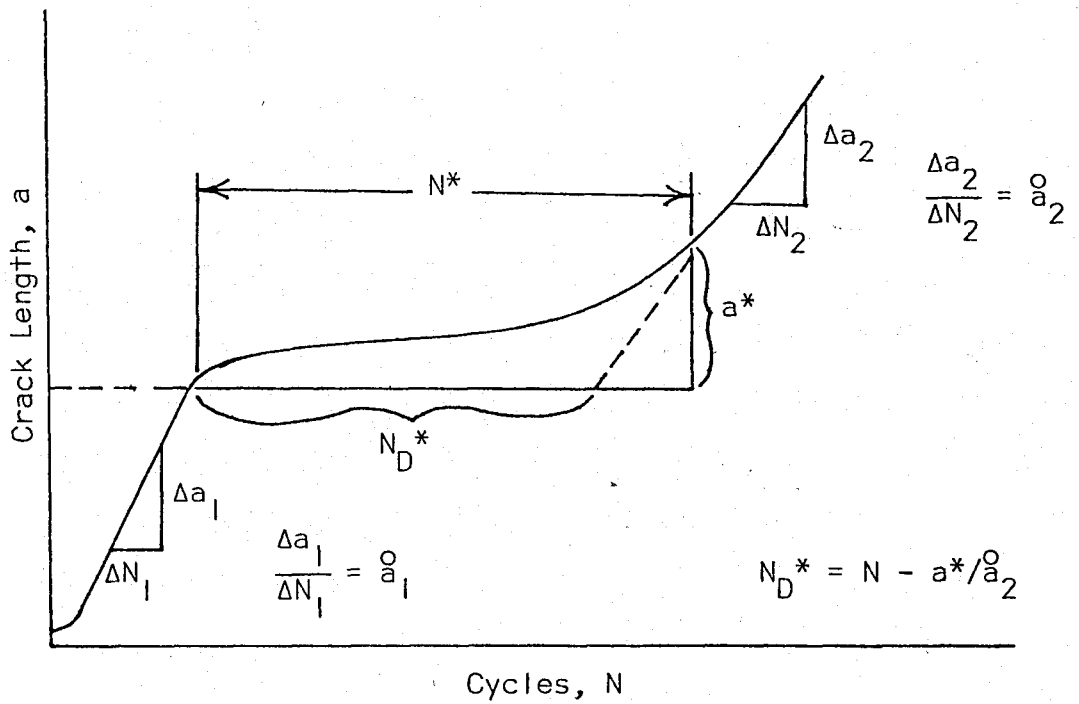


FIGURE 8. SCHEMATIC OF A GROWTH RATE CURVE RESULTING FROM A SINGLE OVERLOAD.

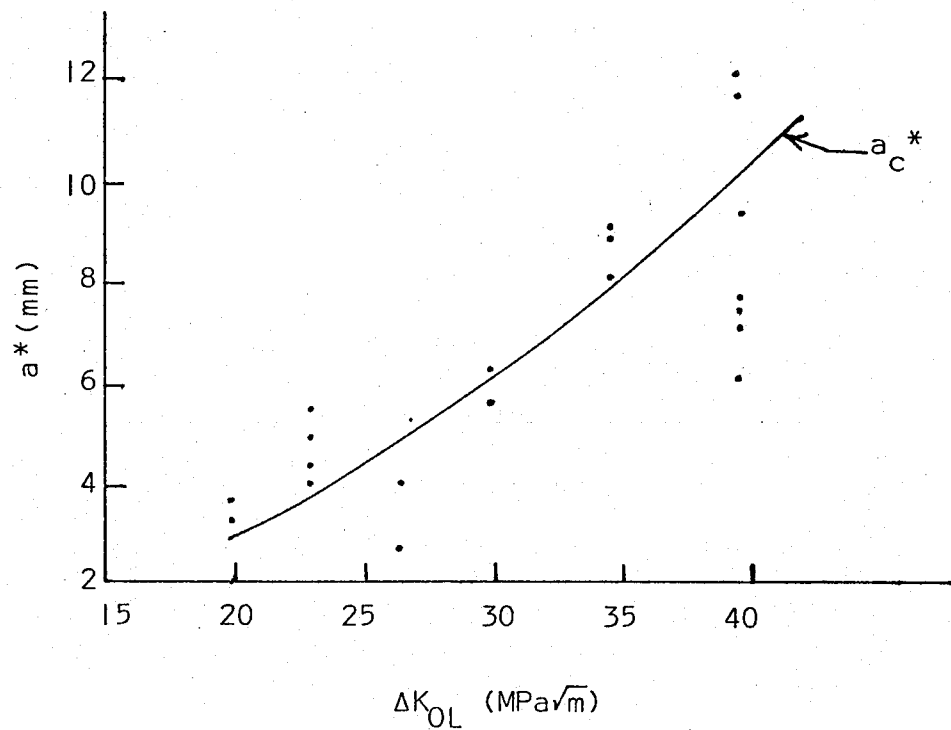


FIGURE 9. COMPARISON OF a^* AND a_c^* .

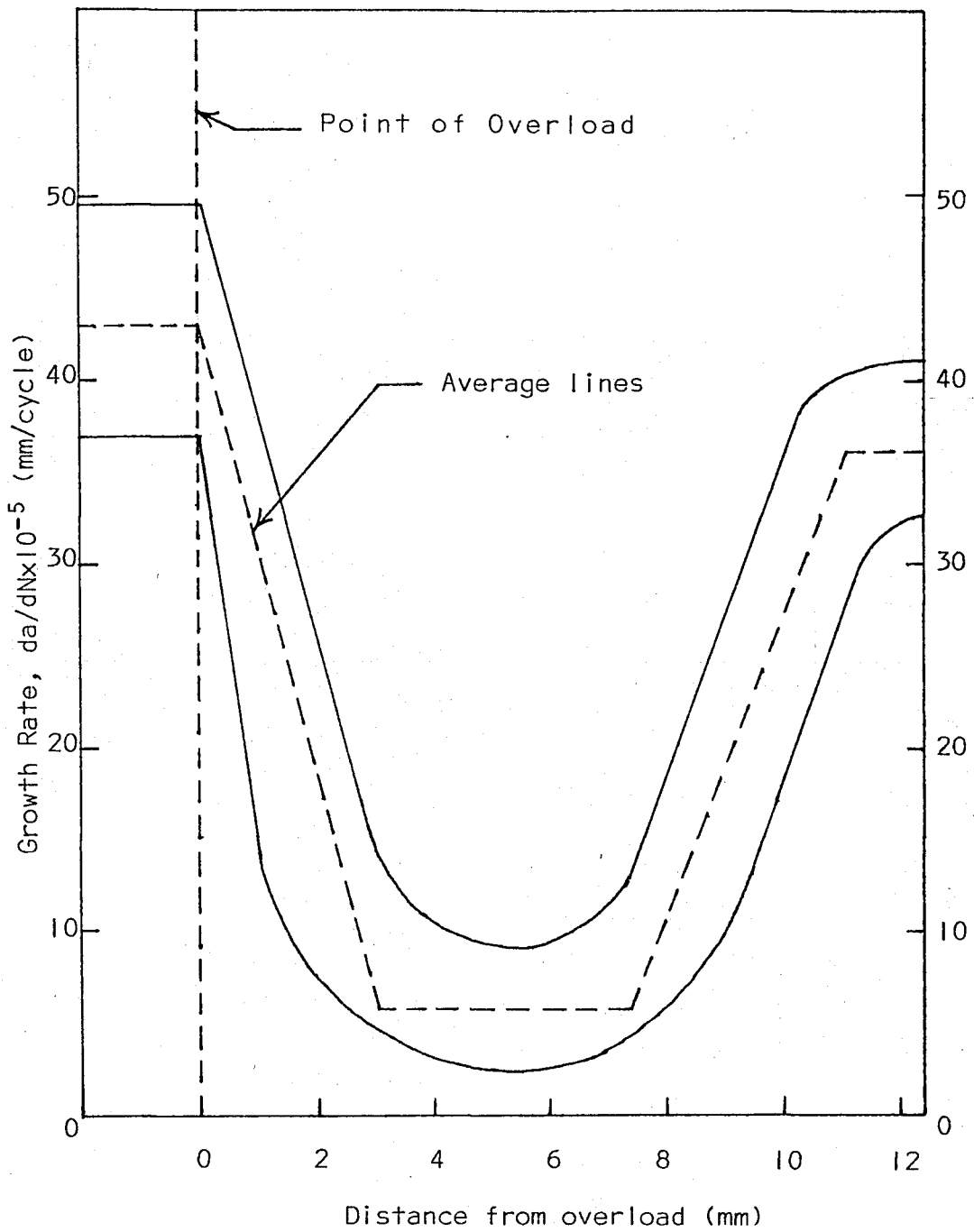


FIGURE 10. BAND OF GROWTH RATE-DISTANCE FROM OVERLOAD RESULTS WITH AVERAGE LINES THROUGH MIDDLE.

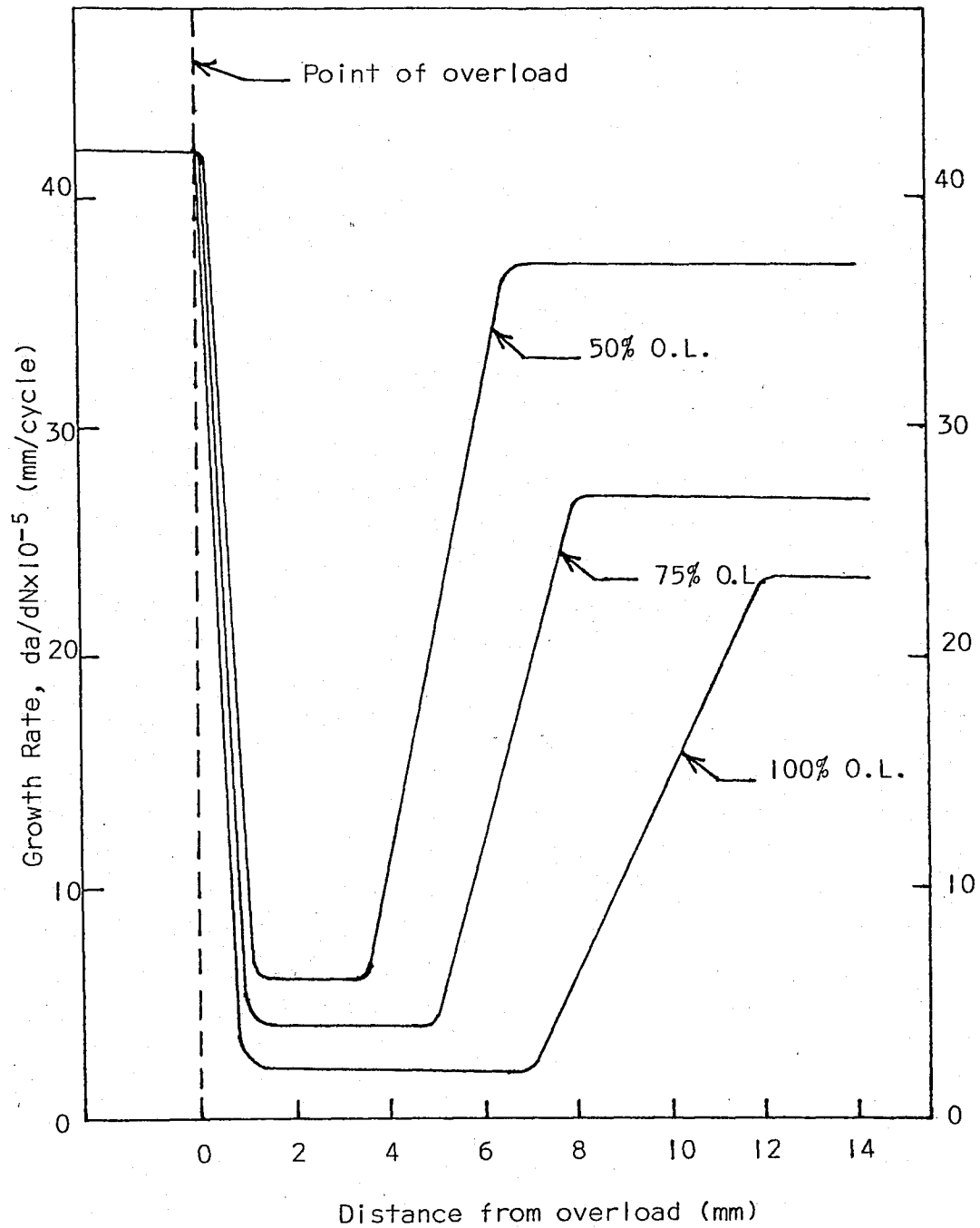


FIGURE 11. COMPARISON OF GROWTH RATE VS. DISTANCE FROM OVERLOAD RESULTS FOR 50, 75, AND 100 PERCENT OVERLOADS

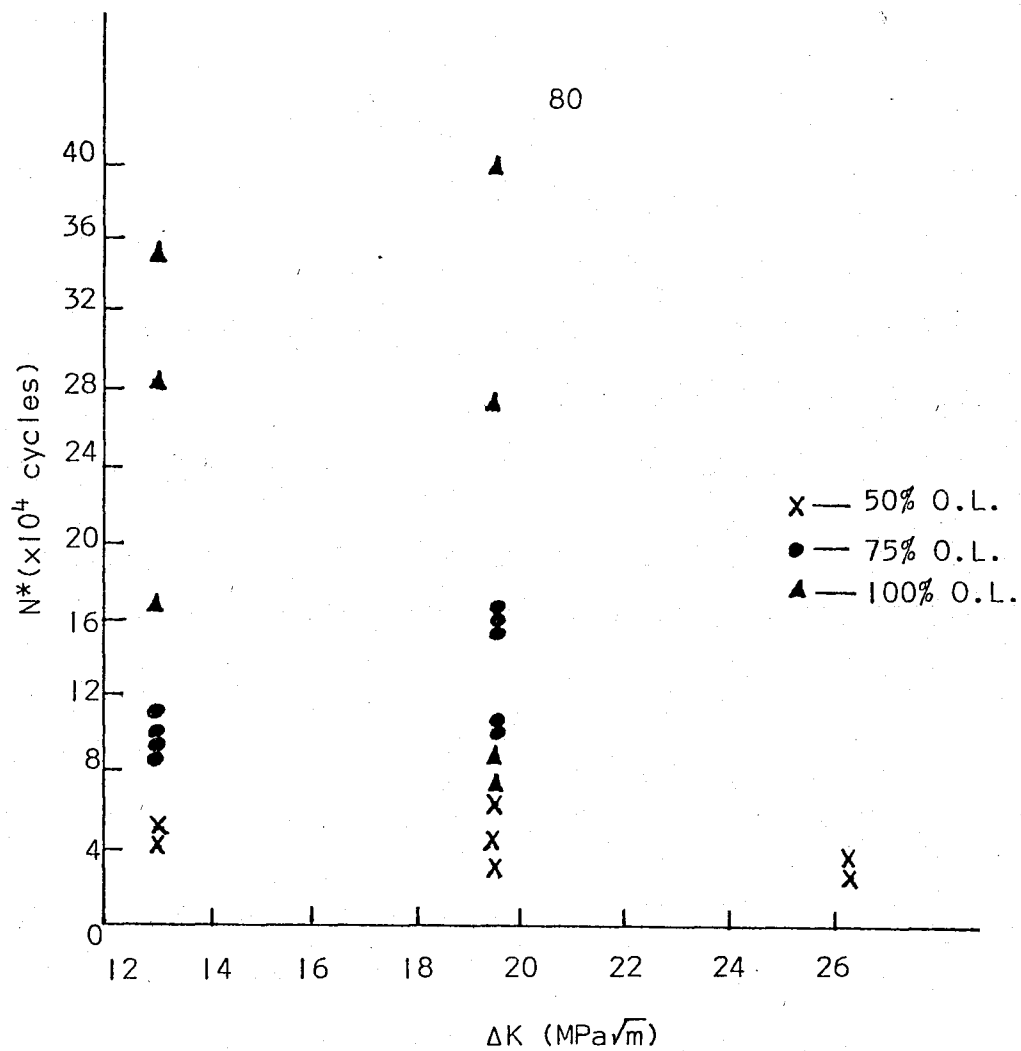


FIGURE 12. CYCLES OF DELAY VERSUS ΔK LEVEL FOR 50, 75, AND 100 PERCENT OVERLOADS.

REFERENCES

1. Christensen, R. H. and Harmon, M. B. in Fatigue Crack Propagation, ASTM STP 415, American Society for Testing and Materials, 1967, p. 5.
2. Paris, P. C. and Erdogan, F., Journal of Basic Engineering, ASME, Series D of the Transactions of the American Society of Mechanical Engineers, 1963, p. 528.
3. Trebules, V. W., Jr., Roberts, R., and Hertzberg, R. W., "Effect of Multiple Overloads on Fatigue Crack Propagation in 2024-T3 Aluminum Alloy", Progress in Flaw Growth and Fracture Testing, ASTM STP 536, ASTM, 1973, pp. 115-146.
4. von Euw, E. F. J., Hertzberg, R. W., and Roberts, Richard, "Delay Effects in Fatigue Crack Propagation", Stress Analysis and Growth of Cracks, Proceedings of the 1971 National Symposium on Fracture Mechanics, Part I, ASTM STP 513, American Society for Testing and Materials, 1972, pp. 230-259.
5. Shih, T. T. and Wei, R. P., "Effect of Specimen Thickness on Delay in Fatigue Crack Growth", Journal of Testing and Evaluation, JTEVA, Vol. 3, No. 1, Jan. 1975, pp. 46-47.
6. Mills, W. J., "Load Initiation Effects on Fatigue Crack Growth in 2024-T3 Aluminum and A514F Steel Alloys", a Ph.D. Dissertation, Lehigh University, 1975.
7. Elber, W. in Damage Tolerance in Aircraft Structures, ASTM STP 486, American Society for Testing and Materials, 1971, p. 230.
8. ASTM Standard E399-72, Annual Book of ASTM Standards, 1972.
9. Kelsey, R. A., Nordmark, G. E., and Clark, J. W., "Fatigue Crack Growth in Aluminum Alloy 5083-O Thick Plate and Welds for Liquified Natural Gas Tanks", Fatigue and Fracture Toughness-Cryogenic Behavior, ASTM STP 556, American Society for Testing and Materials, 1974, pp. 159-185.

VITA

Kenneth A. Wnek was born the son of Arthur H. and Stella Wnek on March 15, 1953 in Newark, New Jersey. He received his elementary and secondary education from the Hanover Township School System of New Jersey, and was graduated from Whippany Park High School in 1971.

In June 1975 the author was graduated from Lehigh University with the degree of Bachelor of Science in Mechanical Engineering. While at Lehigh, Mr. Wnek was a member of the ASME and won second place in the 1975 ASME Papers contest with a presentation entitled "Delay of Fatigue Crack Propagation".

Since 1975 the author has continued his education as a Research Assistant in the Mechanical Engineering Department at Lehigh under the supervision of Dr. Richard Roberts. He now plans to gain employment in the field of Fracture Mechanics.